Cell Reports
Medicine

Article

MicroRNA-dependent suppression of biological pacemaker activity induced by TBX18

Graphical abstract

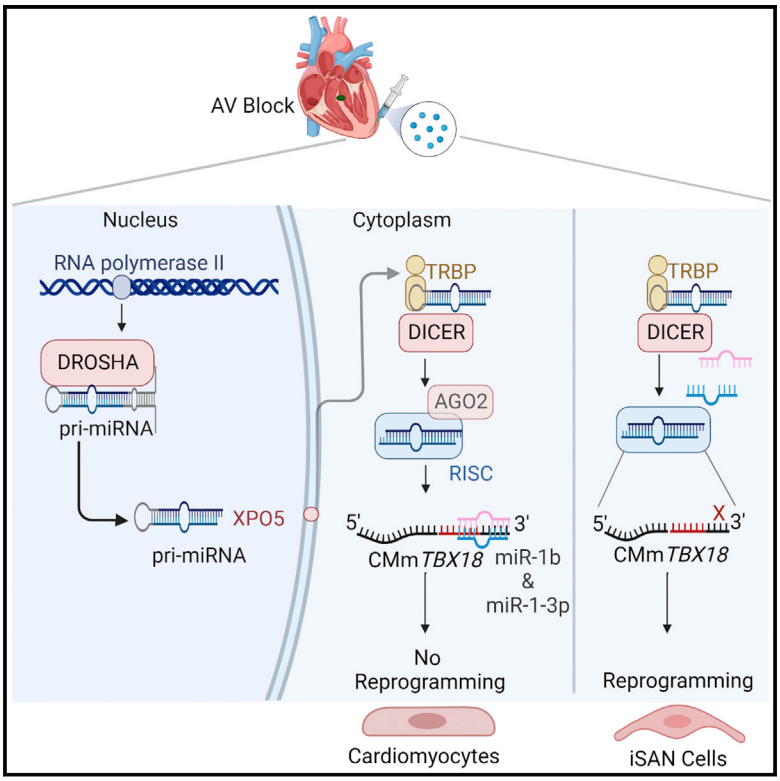

Highlights

- Chemically modified mRNA translation is suppressed by endogenous microRNAs
- Blockade of suppressive microRNAs enhance transgene expression and biological activity
- Sustained translation of TBX18 results in biological pacing activity

Authors

Lizbeth Sanchez, Thassio Mesquita, Rui Zhang, ..., Kevin Holm, Eduardo Marbán, Eugenio Cingolani

Correspondence

eugenio.cingolani@csmc.edu

In brief

Sanchez et al. show that a chemically modified mRNA encoding human TBX18 is suppressed by microRNAs *in vitro* and *in vivo*. Counterstrategies that block suppressive microRNA function led to robust TBX18 protein expression and the generation of electrical stimuli that mimic pacemaker cells in a rat model of atrioventricular block.

Sanchez et al., 2022, Cell Reports Medicine *3*, 100871
December 20, 2022
https://doi.org/10.1016/j.xcrm.2022.100871

CellPress

Cell Reports Medicine

CellPress
OPEN ACCESS

Article

MicroRNA-dependent suppression of biological pacemaker activity induced by TBX18

Lizbeth Sanchez,[1] Thassio Mesquita,[1] Rui Zhang,[1] Ke Liao,[1] Russell Rogers,[1] Yen-Nien Lin,[1] Rodrigo Miguel-dos-Santos,[1] Akbarshakh Akhmerov,[1] Liang Li,[1] Asma Nawaz,[1] Kevin Holm,[1] Eduardo Marbán,[1] and Eugenio Cingolani[1,2,*]

[1]Smidt Heart Institute, Cedars-Sinai Medical Center, 127 S San Vicente Blvd, Los Angeles, CA 90048, USA

[2]Lead contact

*Correspondence: eugenio.cingolani@csmc.edu

https://doi.org/10.1016/j.xcrm.2022.100871

SUMMARY

Chemically modified mRNA (CMmRNA) with selectively altered nucleotides are used to deliver transgenes, but translation efficiency is variable. We have transfected CMmRNA encoding human T-box transcription factor 18 (CMm*TBX18*) into heart cells or the left ventricle of rats with atrioventricular block. TBX18 protein expression from CMm*TBX18* is weak and transient, but Acriflavine, an Argonaute 2 inhibitor, boosts TBX18 levels. Small RNA sequencing identified two upregulated microRNAs (miRs) in CMm*TBX18*-transfected cells. Co-administration of miR-1-3p and miR-1b antagomiRs with CMm*TBX18* prolongs TBX18 expression *in vitro* and *in vivo* and is sufficient to generate electrical stimuli capable of pacing the heart. Different suppressive miRs likewise limit the expression of VEGF-A CMmRNA. Cells therefore resist translation of CMmRNA therapeutic transgenes by upregulating suppressive miRs. Blockade of suppressive miRs enhances CMmRNA expression of genes driving biological pacing or angiogenesis. Such counterstrategies constitute an approach to boost the efficacy and efficiency of CMmRNA therapies.

INTRODUCTION

Beginning during embryonic development and continuing throughout a typical human lifespan, the heart beats, on average, more than 3 billion times. This remarkable activity is made possible by the heart's endogenous pacemaker, which spontaneously generates rhythmic electrical impulses to initiate every beat of the heart. The primary pacemaker of the heart resides in the sinoatrial node (SAN) and is responsible for setting the frequency at which the heart beats.[1] Specialized "nodal" cells in the SAN express HCN4, which enables pacemaker current—otherwise known as the funny current (I_f).[2] Failure of the SAN to generate electrical impulses and/or conduction system disturbances, which impede normal propagation, results in slow heart rhythm or bradycardia. As a result, electrical pacemakers have become a mainstay in therapeutic intervention for slow heart rhythms resulting from conduction system disease.[3] Although 6 decades of contemporary innovations have greatly improved the safety and efficacy of implantable electrical pacemakers, several challenges remain that warrant the development of alternative therapeutic strategies.[1]

One such promising approach has been the development of a *de novo* biological pacemaker, which conceptually creates an ectopic region of automaticity that can function as a surrogate for the SAN. Several cell- and gene-based approaches have been evaluated[4–6]; however, translating these approaches to the clinic remains a challenge. With a view of clinical translation, rather than functional reengineering approaches, somatic reprogramming seeks to transfer genes encoding transcription factors that create bona fide replicas of genuine pacemaker cells. We have previously shown that transfer of human embryonic T-box transcription factor 18 (TBX18) converts cardiomyocytes into induced SAN (iSAN) cells, which biochemically and functionally resemble endogenous SAN pacemaker cells.[7] Moreover, *in vivo* somatic reprogramming by viral delivery of TBX18 created a biological pacemaker rhythm that not only originated at the injection site but also responded to catecholamines.[7]

Viral vectors have been commonly used to deliver transgenes *in vitro* and *in vivo*, and they can be tailored to enhance cardiac gene transfer.[8] Nevertheless, viral vectors have disadvantages including the potential for a host immune response to viral proteins and/or insertional mutagenesis. One alternative is direct delivery of transgene mRNA,[9] which circumvents the risk of insertional mutagenesis by genomic integration from viral vectors and facilitates rapid protein expression.[10,11] While naked RNA elicits immune activation,[12–14] mRNA can be chemically modified (CMmRNA) using nucleosides such as pseudouridine (Ψ), 5-methylcytidine (m5C), or 2-thiouridine (s2U) to avoid immune activation and enhance translation.[15–17]

Here, we modified uridine residues in human *TBX18* mRNA (CMm*TBX18*) with 1-methylpseudouridine-5′-triphosphate (1-mψU).[16] A single transfection with CMm*TBX18* induces transient protein expression for 24 h in neonatal rat ventricular myocytes (NRVMs), which could not be sustained beyond 24 h

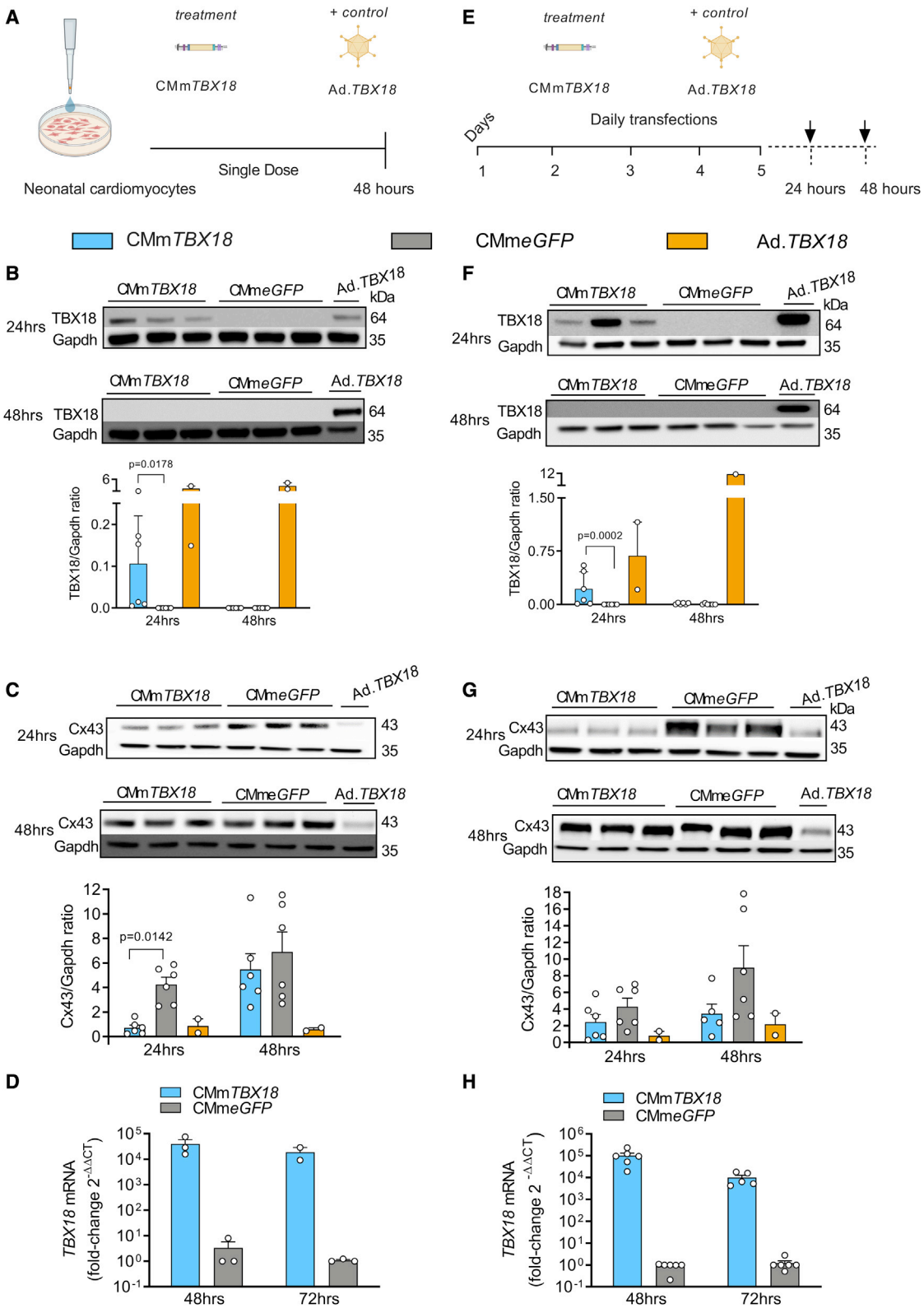

(legend on next page)

even by repeated dosing. Mechanistically, we discovered that microRNAs (miRs) suppress translation of CMm*TBX18* and devised counterstrategies that led to sustained protein expression and enhanced disease-modifying bioactivity. We also showed that this phenomenon is not specific to chemical modification selection nor the TBX18 transgene, which may have important implications for generalized use of CMmRNA.

RESULTS AND DISCUSSION

In vitro TBX18 transgene expression by CMm*TBX18*

Adenovirally mediated delivery of TBX18[7,18] can reprogram ventricular cardiomyocytes into iSAN cells *in vitro* and *in vivo,* creating a biological pacemaker. However, long-term efficacy is limited by immunological clearance of transduced cells.[7] To circumvent viral vector limitations, we investigated CMmRNA as an alternative means of delivering the *TBX18* transgene (CMm*TBX18*; Figure 1A). Transfection of NRVMs with 1-mψU CMm*TBX18*[16] yielded detectable levels of TBX18 protein at 24 h (Figure 1B) (unlike *EGFP* CMmRNA-transfected controls [CMm*EGFP*]), as did a TBX18-expressing adenovirus (Ad.*TBX18*).[7] The expression of TBX18 protein was short lived, however, no longer being detectable 48 h post-transfection with CMm*TBX18* (unlike Ad.*TBX18*, which expresses protein even more strongly at 48 h than at 24 h; Figure 1B). Because TBX18 decreases Cx43 expression in heart cells,[19] Cx43 expression levels reciprocally index TBX18 function. Consistent with the transient time course of TBX18 expression by CMm*TBX18*, Cx43 protein levels were reduced at 24 h but returned to baseline by 48 h post-transfection (Figure 1C). However, *TBX18* transcripts were abundant at least for 72 h post-transfection, ruling out mRNA decay as the basis of either transient TBX18 expression or transient Cx43 suppression (Figure 1D). Repeated daily transfections with CMm*TBX18* (Figure 1E) were ineffective at sustaining TBX18 expression beyond 24 h (Figure 1F); meanwhile, Cx43 was downregulated only at 24 h (Figure 1G), although *TBX18* transcripts were abundant at 48 h (Figure 1H).

Blockade of Argonaute 2 permits persistent TBX18 protein expression

Having excluded mRNA decay as a major contributor, we hypothesized that translational suppression may foreshorten protein expression. Acriflavine (ACF), a small-molecule inhibitor of Argonaute 2 (AGO2) function[20,21]—which binds small non-coding RNAs (including miRs) and guides them to their mRNA targets through sequence complementarity at the 3′ UTR.[22] The AGO-miR-mRNA complex then interferes with ribosomal function at the 5′ end of the mRNA to suppress translation[22,23] (Figure 2A). In NRVMs exposed to ACF 24 h before transfection, TBX18 protein levels were more robust, and expression was sustained for at least 72 h following a single transfection with CMm*TBX18* but not CMm*EGFP* (Figure 2B). Consistent with sustained TBX18 expression, Cx43 remained downregulated for at least 72 h (Figure 2C). To test if similarly transient protein expression was seen with other nucleoside modifications, we substituted uridine with 5-methoxyuridine (5moU) to create CMm*TBX18*. TBX18 protein expression was undetectable at either 24 or 48 h (Figure S1A), but after pre-treatment with ACF, expression was robustly sustained for at least 72 h (Figure S1B). These data support the idea that miRs (and not mRNA decay [Figure S1C]), whether constitutively expressed or upregulated in response to CMm*TBX18*, suppress TBX18 protein expression in NRVMs regardless of the specific mRNA chemical modification.

miR-1-3p and miR-1b arrest CMm*TBX18* translation

The rescue of TBX18 expression by ACF implicates miRs in the mechanism of suppression. Indeed, the miRNome of NRVMs was markedly altered after transfection with CMm*TBX18* (Figure 2D). Two of the most highly upregulated miRs (miR-1-3p and miR-1b; Figure 2E) share sequence complementarity with the *TBX18* 3′ UTR (Table S1). To test whether miR-1-3p and/or miR-1b inhibit *TBX18*, we performed a luciferase miR binding assay. Indeed, miR-1-3p and miR-1b suppress luciferase activity, directly demonstrating that these miRs bind *TBX18* 3′ UTR and suppress translation (Figure 2F). Co-transfection of NRVMs with CMm*TBX18* and antagomiRs to miR-1-3p and miR-1b led to sustained TBX18 protein expression for at least 48 h (Figure 2G) and HCN4 protein expression at 72 h (Figure 2H).

To assess the functional consequences for cellular electrophysiology, we used whole-cell patch clamp to phenotype NRVMs transfected with CMmGFP or CMmTBX18. Supporting somatic reprogramming, CMmTBX18-transfected NRVMs showed typical action potential (AP) morphology of pacemaker-like cells, while the AP morphology of CMmEGFP-transfected NRVMs was that

Figure 1. *In vitro TBX18* transgene expression of chemically modified mRNA

(A) Experimental overview of the transfection protocol used to induce transgene expression in NRVMs.

(B) Representative western blot demonstrating TBX18 protein expression 24 and 48 h post-transfection (left). Quantification by densitometry analysis (bottom) (n = 6 in each experimental group and n = 2 in *TBX18* adenovirus [biological replicates]).

(C) Representative western blot demonstrating Cx43 protein expression 24 and 48 h post-transfection. Quantification by densitometry analysis (bottom) (n = 6 in each experimental group and n = 2 in *TBX18* adenovirus [biological replicates]). Adenovirus expressing TBX18 was used as positive control (tan bars).

(D) Quantitative reverse-transcriptase PCR (qRT-PCR) indicated that *TBX18* mRNA expression declined between 48 and 72 h (n = 3 in each experimental group [biological replicates]) in a single dosing.

(E) Experimental overview depicting repeated transfection protocol in NRVMs.

(F) Representative western blot demonstrating TBX18 expression 24 and 48 h following the last dose (right). Quantification by densitometry analysis (bottom) (n = 6 in each experimental group and n = 2 in *TBX18* adenovirus [biological replicates]).

(G) Representative western blot demonstrating Cx43 protein expression 24 and 48 h following the last dose. Quantification by densitometry analysis (n = 6 in each experimental group and n = 2 in *TBX18* adenovirus [biological replicates]).

(H) qRT-PCR indicated that *TBX18* mRNA expression declined between 48 and 72 h (n = 6 in each experimental group [biological replicates]) in repeated transfections.

Data are represented as mean ± SEM. Statistical significance was determined using an independent t test.

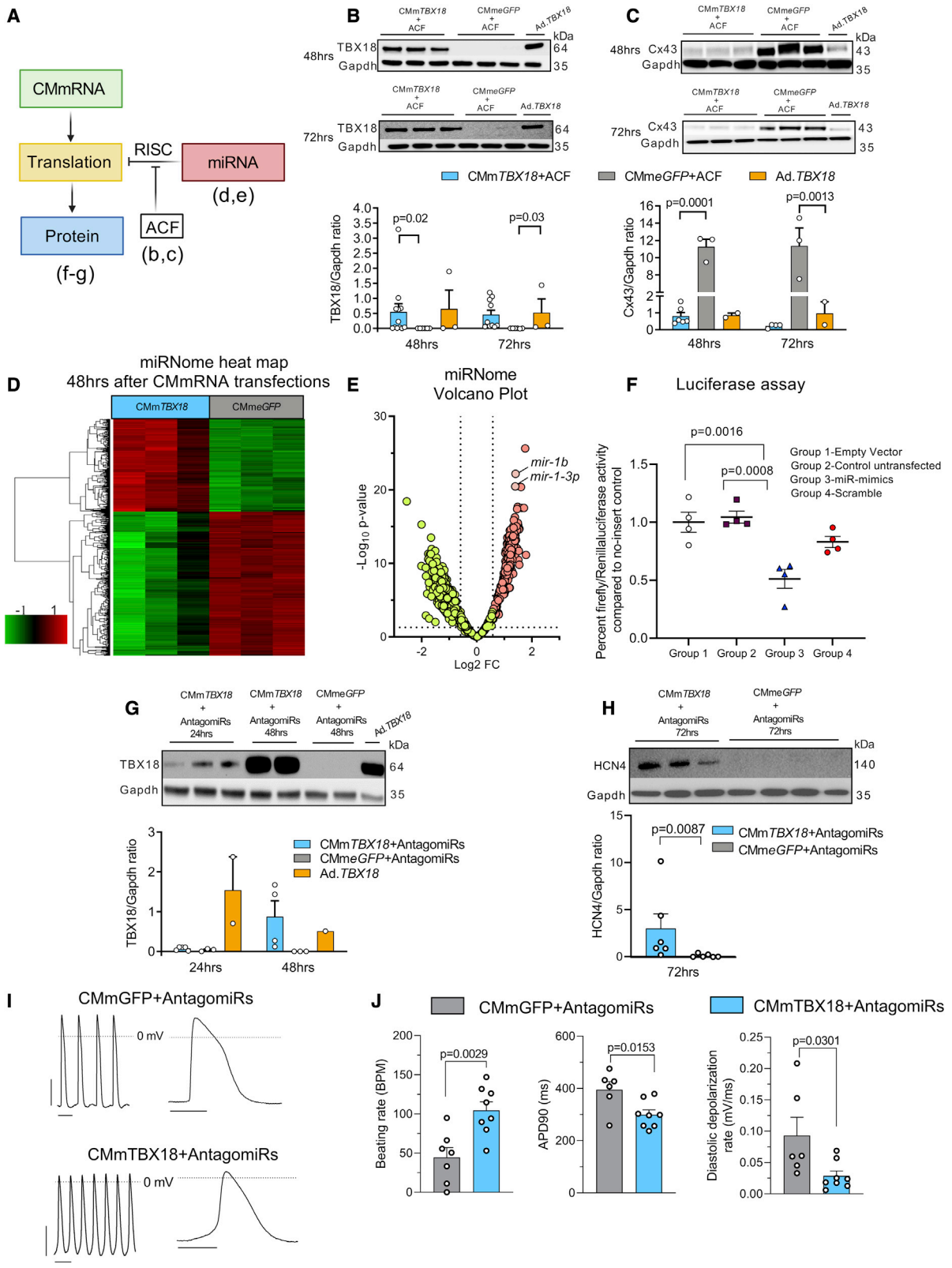

(legend on next page)

of working cardiomyocytes (Figure 2I). These morphological AP modifications seen in CMmTBX18-NRVMs reproduce those that underlie automaticity in pacemaker cells.[1,7] Further bolstering the idea that we have induced pacemaker activity, transduction with CMmTBX18 and both antagomiRs increased beating rate, abbreviated AP duration at 90%, and slowed diastolic depolarization (Figure 2J). However, co-transfection with one or the other antagomiR alone failed to sustain TBX18 protein expression (Figures S2A and S2B). NRVMs co-transfected with CMm*TBX18* and the two antagomiRs demonstrated distinctive iSAN morphology 72 h post-transfection, which was associated with HCN4 and HCN2 protein expression by immunocytochemistry, consistent with somatic reprogramming like that induced by Ad.*TBX18*.[7] Moreover, changes in gene expression (HCN2, HCN4, SCN5a, and Nkx2.5) consistent with somatic reprogramming were also seen at the transcript level (Figures S3A–S3C). Such reprogramming remained durable for at least 1 week post-transfection with CMm*TBX18* and the two antagomiRs (Figures S4A–S4C). These changes in cell morphology were not observed when CMm*TBX18* was transfected without antagomiRs. Together, these data identify miR-1-3p and miR-1b as mediators of *TBX18* transgene suppression. Sustained and robust TBX18 expression can be achieved by combined selective inhibition of these two miRs.

Biological pacemaker activity originates at the CMm*TBX18* injection site

Our interest in CMm*TBX18* originated from a desire to create biological pacemakers without viral vectors. Focal injection of CMm*TBX18* alone into the hearts of rats did not yield biological pacemaker activity (Figures S5A–S5E). Nevertheless, a cocktail containing CMm*TBX18* and miR-1-3p and miR-1b antagomiRs resulted in *de novo* biological pacemaker activity, as revealed by simultaneous field electrocardiography (ECG) and optical mapping of hearts excised 72 h post-injection (Figures 3A–3E). After induction of complete atrioventricular (AV) block, ECG recordings showed the QRS duration of ventricular escape beats to be prolonged in both CMm*TBX18* and CMm*EGFP* groups (Figure S6A). However, the time to first ventricular escape beat (a measure of excitability) was shorter, and the frequency of ventricular escape beats was higher, in CMm*TBX18*-transfected hearts (Figure 3C), as expected.[24,25] The average heart rate 2 min prior to AV block was not different between groups, nor was atrial beating rate within 2 min after AV block (Figure 3D). Nevertheless, the ventricular rate after AV block was higher in CMm*TBX18*-transfected hearts than in control hearts (Figure 3D). Further confirming the functionality of induced biological pacemakers, ectopic ventricular beats originated at the injection site in CMm*TBX18*-transfected hearts[26] (Figure 3E). Sinus node-like APs were also found within the injection site in CMm*TBX18*-transfected hearts but neither in remote sites nor in control hearts[24] (Figure 3E). At the biochemical level, *TBX18* mRNA was present (and increased) at the injection site after CMm*TBX18* and dual antagomiR co-injection, and genes known to be influenced by TBX18 (Cx43, SCN5a, and Nkx2.5)[7] were appropriately altered (Figure 3F). TBX18 immunohistochemistry revealed iSAN morphology of cells at the injection site, but control hearts showed only rod-shaped conventional ventricular myocytes[7,24] (Figure 3G). To test the durability of TBX18 expression and reprogamming, we transfected rat hearts with CMm*TBX18* and the two antagomiRs, then analyzed the hearts 2 weeks later (Figures S7A–S7E). The expected changes in electrical activity following AV block were observed (Figures S7B and S7C). While TBX18 mRNA expression and protein expression were decreased, reprogramming markers such as HCN4, HCN2, and Cx45 were sustained at the protein level by immunohistochemistry (Figure S8A). Together, these data indicate that CMm*TBX18* is effective *in vivo* but only when co-delivered with antagomiRs to miR-1-3p and miR-1b, inducing local iSAN cells and *de novo* biological pacemaker activity.

Figure 2. Argonaute 2-dependent suppression of TBX18 protein expression: miR-1-3p and miR-1b arrest *TBX18* mRNA translation

(A) Schematic representation of the RNA-induced silencing complex and Argonaute 2 (AGO2)-dependent TBX18 protein suppression. AGO2 binds to the cytosolic miRNA-processing machinery and complementary *TBX18* mRNA at the 3′ UTR. Acriflavine (ACF) inhibits AGO2 function in mammalian cells.

(B) Representative western blot demonstrating sustained TBX18 protein expression up to 72 h post-transfection (single dose) by 2.5 μM ACF (top right). Quantification by densitometry analysis (bottom) (n = 12 in 48 h CMm*TBX18* + ACF; n = 10 in 72 h CMm*TBX18* + ACF; n = 6 in 48 h CMm*EGFP* + ACF; n = 6 in 72 h CMm*EGFP*; n = 3 in 48 h *TBX18* adenovirus; and n = 2 in 72 h *TBX18* adenovirus [biological replicates]).

(C) Representative western blot demonstrating downregulated Cx43 protein expression up to 72 h post-transfection (top right). Quantification by densitometry analysis (bottom) (n = 12 in each experimental group and n = 2 in *TBX18* adenovirus [biological replicates]).

(D and E) (D) miRNome heatmap analysis of miRNA expression demonstrates a robust change 48 h after transfection with *TBX18* chemically modified mRNA (middle left). (E) Volcano plot representing the most upregulated and downregulated miRs indicate that miR-1-3p and miR-1b are highly upregulated after *TBX18* chemically modified RNA transfection. Prediction analysis demonstrating that miR1-3p and miR-1b are predicted to bind to TBX18 3′ UTR (centered).

(F) Representative TBX18 3′ UTR luciferase assay results quantified by percentage of firefly/Renilla luciferase activity compared with no-insert control. Experimental conditions were as follows: group 1, empty vector; group 2, control untransfected; group 3, miR-1-3p/miR-1b mimc transfections; and group 4, a scramble sequence transfection (bottom right) (n = 4 in empty vector; n = 4 in control untransfected; n = 4 in miR-1-3p/miR-1b mimic treatment; and n = 4 in scramble sequence [biological replicates]).

(G and H) Representative western blot demonstrating sustained TBX18 protein expression by co-transfecting NRVMs with *TBX18* chemically modified RNA and antagomiRs to miR-1-3p and miR-1b (bottom left). Quantification by densitometry analysis (bottom) (n = 4 in *TBX18*, n = 2 in *EGFP* chemically modified mRNA, and n = 2 in *TBX18* adenovirus [biological replicates]). Adenovirus expressing a *TBX18* transgene was used as a positive control in (H). Representative western blot demonstrating HCN4 protein expression by co-transfecting NRVMS with *TBX18* chemically modified RNA and antagomiRs to miR-1-3p and miR-1b (bottom middle). Quantification by densitometry analysis (bottom) (n = 6 in *TBX18* and n = 6 in *EGFP* [biological replicates]).

(I) Representative action potential traces from CMmEGFP- or CMm*TBX18*-treated NRVMs highlighting the gradual phase 4 depolarization in CMm*TBX18*.

(J) Beating rate, action potential duration at 90% (APD90), and depolarization rate of the membrane potential are summarized.

Data are represented as mean ± SEM. Statistical significance was determined using an independent t test.

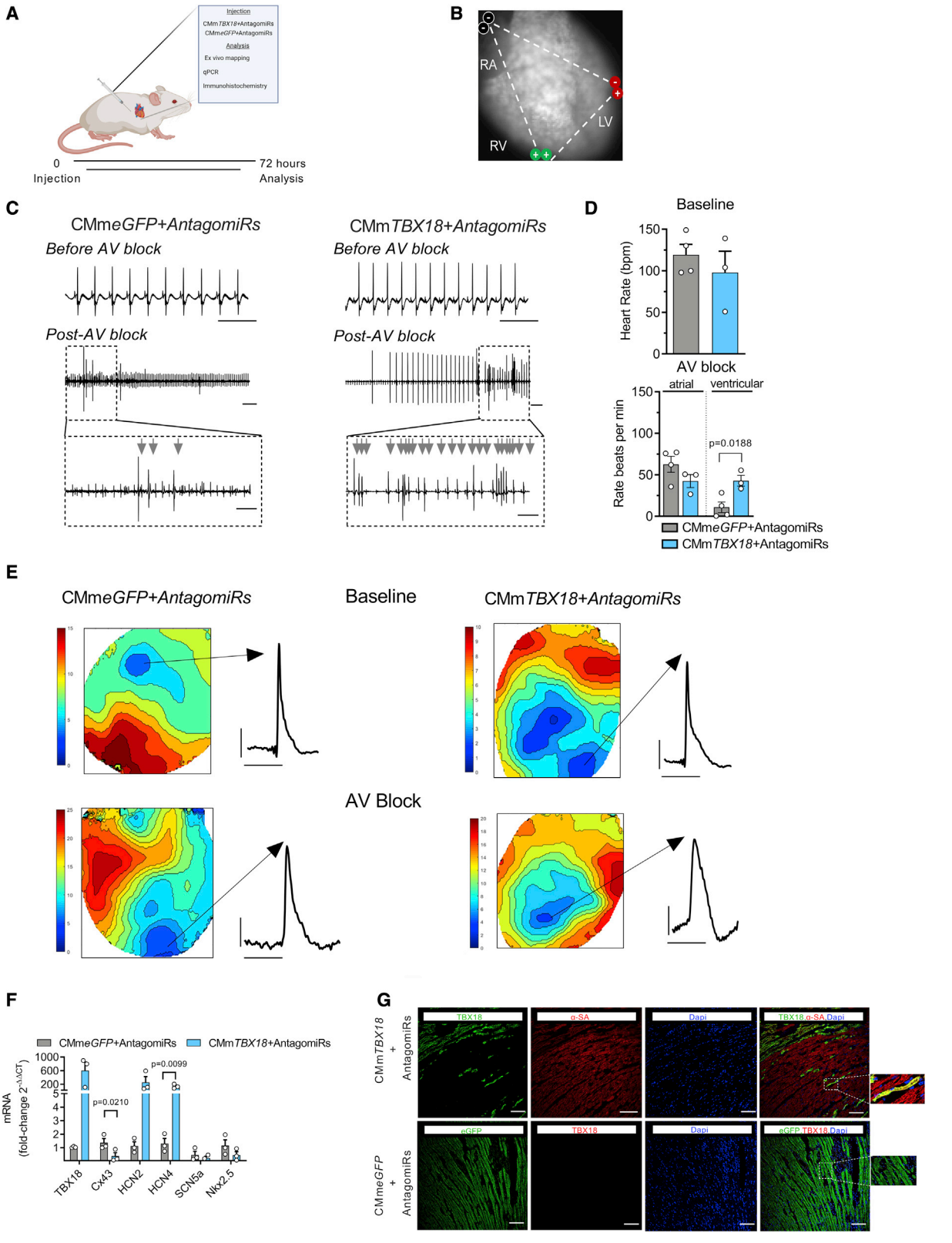

(legend on next page)

Universality of miR-dependent CMmRNA translation suppression

To assess whether miR-induced suppression of CMmRNA is generalizable, we transfected CMmRNA (using the 1-mψU chemical modification) encoding a completely unrelated therapeutic transgene, vascular endothelial growth factor A (CMm*VEGF-A*), in NRVMs. After 24 h, VEGF-A protein expression was downregulated, but this deficit was cured by co-administration of ACF (Figures 4A and 4B). As with CMm*TBX18*, changes in mRNA decay could not explain the low VEGF-A protein levels (Figure 4C). Likewise, miR sequencing (miR-seq) identified robust changes in the NRVM miRNome in response to CMm*VEGF-A* (Figure 4D), but these were entirely distinct from the changes induced by CMm*TBX18*. Alignment of upregulated miRs to the *VEGF-A* 3′ UTR (Table S1) identified several miRs (let-7f-2-3p, miR-106b-5p, miR-208a-3p, miR-34b-5p, miR-138-1-3p, and miR-6316) as potential candidates. To validate this prediction, we performed a luciferase miR binding assay. Indeed, miR-106b-5p suppress luciferase activity, directly demonstrating this miR binds *VEGF-A* 3′ UTR and suppresses translation (Figure 4F). Co-transfection of NRVMs with CMm*VEGF-A* and a cocktail containing antagomiRs to each of these identified miRs led to sustained VEGF-A protein expression for at least 72 h (Figure 4G). When each of the antagomiRs was tested individually, only miR-6316 led to sustained VEGF-A protein expression (Figures 4E, S9A, and S9B). However, the functional significance of the changes in VEGF-A are less clear than with TBX18, as transient expression of VEGF-A by CMmRNA, without adjunctive modifiers, suffices for therapeutic benefits.[15,27] Nevertheless, VEGF-A expression can be boosted and prolonged by adding ACF or anti-miR-6316, which may enable dose reduction and/or prolongation of interdosing intervals to achieve comparable angiogenic benefits.

Here, we have shown that cardiomyocytes "fight back" against the expression of proteins encoded by two very different CMmRNAs of cardiovascular relevance: TBX18, which reprograms ventricular cells into iSAN pacemaker cells; and VEGF-A, which mediates angiogenesis. In response to transfection, the heart cells deploy very specific miRs that specifically counter the expression of each therapeutic CMmRNA. By inhibiting AGO2, or by using focused antagomiRs, we achieved robust, sustained protein expression of either transgene. In the case of TBX18, the anti-suppressive therapy was critical in unleashing biological pacemaker activity, making a decisive difference in disease-modifying bioactivity.

Due to risks and complications of viral-mediated gene delivery,[1] alternatives such as direct delivery of mature mRNA are potentially attractive.[16,28] Transfections of mRNA induce rapid transgene expression with no risk of insertional mutagenesis.[9] Because non-modified mRNAs are susceptible to cleavage by RNase and rapid immune clearance when delivered *in vivo*, nucleoside modifications have been used to stabilize mRNA.[9,15,16] In particular, substitution of cytidine and uridine residues with m5C and ψ, respectively, promotes more efficient translation while minimizing immunogenic responses and resistance to RNase.[10,11,13,15–17,29] CMmRNA has been used to reprogram human fibroblasts into induced pluripotent stem cells (iPSCs)[30] and increase telomerase activity in fibroblasts and myoblasts.[31] In earlier studies, suppression of protein expression following delivery of CMmRNA was also observed,[32,33] and co-transfection of CMmRNA with miRs boosts cellular reprogramming (a finding distinct from those reported here)[32,33]; however, long-term transgene expression ultimately requires repeated delivery of CMmRNA.[12] The requirement for repeated transfections to maintain transgene expression, as reported in these studies, can be a significant barrier to clinical translation.

Because suppression of miR-1-3p can aggravate cancer,[34–37] we investigated the safety of our therapeutic cocktail *in vitro* and *in vivo*. Three different cancer cell lines (lung adenocarcinoma, A549; liver cancer, 769-p; and ovarian cancer, SKOV-3) were transfected with CMm*TBX18* and miR cocktail mimics and inhibitors. No increased pro-metastatic activity was seen in most of the cell lines (some migratory activity in SKOV-3 cells), as assessed by Transwell migration assay and proliferation by EdU staining (Figures S10A–S10D and S11A–S11D). Next, we delivered our cocktail into Sprague-Dawley rats and assayed mRNA and protein (by immunohistochemistry) expression of oncogenes PFTK1 (CDK14) and E2F5. No changes in these oncogenes were observed at either the mRNA or protein levels (Figures S12A–S12H and S13A–S13H). Further, we assessed tumor formation by H&E staining at 8 weeks after our treatment and found no tumors by gross inspection or histology (Figures S14A and S14B).

Figure 3. *TBX18* chemically modified mRNA biological pacemaker activity originates at the focal injection site and induces iSAN-like morphology in ventricular myocytes *in vivo*

(A) Experimental overview indicating rats were transfected with 100 μg *TBX18* chemically modified mRNA delivered with antagomiRs to miR-1-3p and miR-1b.

(B) A representative fluorescent image with electrodes orientation for far-field electrogram.

(C) Original ECG traces are shown before and after cutting high interventricular septum for induction of permanent AV block (AVB). Note, the time to first ventricular escape beat in the *TBX18* chemically modified RNA-treated group is shorter than that in *EGFP*-treated group. Traces are representative (n = 3 for *TBX18* and n = 4 in *EGFP* chemically modified mRNA [biological replicates]). Scale bars: pre-AVB, 5 s; post-AVB, 20 s; and inset, 80 s.

(D) Average heart rate within 2 min before induction of AVB (n = 3). Average atrial beats within 2 min after induction of AVB (n = 3). Average ventricular beats within 2 min after AVB (n = 3).

(E) Activation maps and action potentials derived from optical mapping are shown after AVB. Arrow indicating the earliest activation site is shown in red. The origin of all ventricular ectopic beats in the *TBX18* chemically modified mRNA-treated group correlated with the injection site. Sinus nodal-like potentials are also found within the injection area in the *TBX18* chemically modified mRNA-treated group. Scale bars: y, 0.25 ms normalized fluorescence units and x, 50 ms. Images are representative (n = 3 for each group [biological replicates]). Hearts were harvested 72 h post-transfection and processed for qRT-PCR and histology.

(F) qRT-PCR demonstrates a 1,000-fold increase in *TBX18* expression at the injection site 72 h post-transfection (n = 3 [biological replicates]).

(G) Immunohistochemical micrographs demonstrate iSAN-like morphology of ventricular myocytes 72 h post-transfection with *TBX18* chemically modified mRNA. Scale bar: 20 μm.

Data are represented as mean ± SEM. Statistical significance was determined using an independent t test.

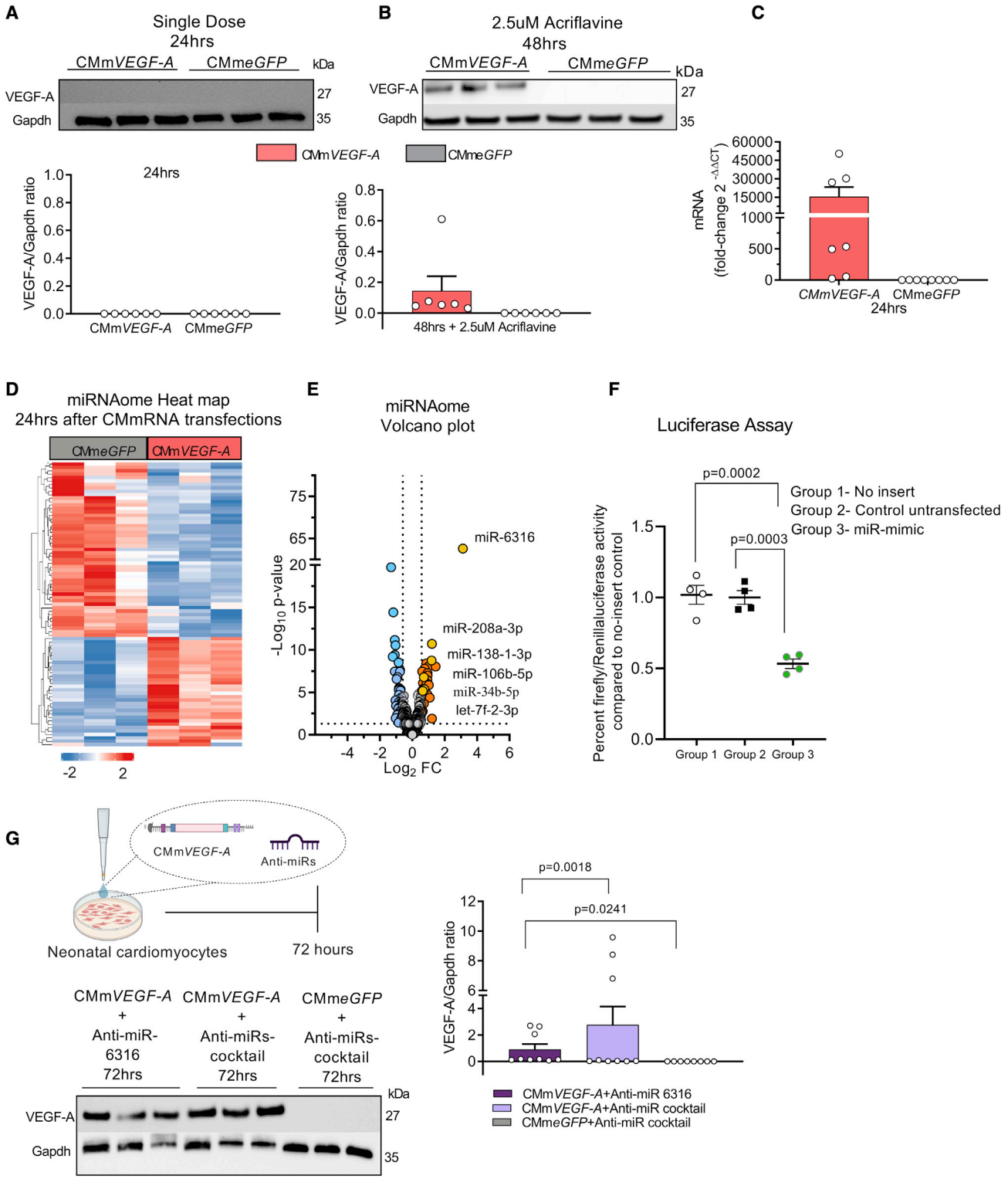

Figure 4. *In vitro* transfection of *VEGF-A* chemically modified mRNA

(A) Representative western blot demonstrating VEGF-A protein expression 24 h post-transfection (top left) (n = 6 per group [biological replicates]).

(B) Representative western blot demonstrating sustained VEGF-A protein expression at 48 h post-transfection by 2.5 μM ACF (top center) (n = 6 [biological replicates]).

(C) qRT-PCR indicated that *VEGF-A* mRNA expression was only seen in *VEGF-A* chemically modified mRNA-treated NRVMS (top right) (n = 7 in *VEGF-A* and n = 8 in *EGFP* chemically modified mRNA [biological replicates]).

(legend continued on next page)

Taken together, our cocktail does not appear to be tumorigenic nor does it aggravate most cancer cell lines.

It is currently unclear whether virally mediated TBX18 protein expression is offset by counteregulatory miRs; in any case, it suffices to achieve the desired function. Here, we have antagonized upregulated miRs or inhibited AGO2. Alternatively, mutating the 3′ UTR seed sequences, or substituting the 3′ UTR with such from a constitutively expressed gene, may circumvent the host cellular response. In any case, not all transgenes are suppressed: our data show that CMm*EGFP* is not subject to counterregulation and thus is translationally privileged. We speculate that, unlike TBX18 and VEGF-A, which alter cell function dramatically, EGFP is inert and thus not subject to counterregulation. Regardless, CMm*EGFP* is not a reliable reporter of functionally active CMmRNA transgene expression. Our findings have conceptual as well as practical value: we not only identify a homeostatic mechanism whereby cells use miRs to resist CMmRNA transgene expression but also pinpoint ways to improve the efficiency of CMmRNA therapeutics.

Limitations of the study

The following limitations should be noted: first, CMmRNA-based approaches have yet to be directly compared with viral-vector-mediated strategies in terms of safety and efficacy. Second, we have demonstrated enhanced reprogramming of ventricular cardiomyocytes to pacemaker cells by inhibiting specific miRs (miR-1-3p and miR-1b), but potential off-target effects have not been fully characterized. Finally, additional studies are needed to assess long-term efficacy and safety to determine the translational potential of this approach.

STAR★METHODS

Detailed methods are provided in the online version of this paper and include the following:

- KEY RESOURCES TABLE
- RESOURCE AVAILABILITY
  - Lead contact
  - Materials availability
  - Data and code availability
- EXPERIMENTAL MODEL AND SUBJECT DETAILS
  - Rats
  - Cells
- METHOD DETAILS
  - Synthesis of TBX18, VEGF-A, and eGFP CMmRNA
  - *In vitro* CMmRNA transfection
  - RNA purification, RT-qPCR analysis, and RNA sequencing
  - Luciferase assay
  - Immunoblotting
  - Single cell electrophysiology
  - 5-Ethynyl-2′-deoxyuridine (EdU assay)
  - Transwell migration assay
  - Immunostaining
  - *In vivo* delivery of *TBX18* CMmRNA
  - *Ex vivo* high-resolution voltage mapping and ECG recordings
- QUANTIFICATION AND STATISTICAL ANALYSIS

SUPPLEMENTAL INFORMATION

Supplemental information can be found online at https://doi.org/10.1016/j.xcrm.2022.100871.

ACKNOWLEDGMENTS

We thank Jeanna Huynh, Nguyenle Hoang, and Lisa Trahan for guidance and editorial support. This work was supported by NHLBI R01-135866 and NHLBI R01-HL147570-04. T.M. was supported by the American Heart Association 836665, and R.M.d.S. was supported by the California Institute for Regenerative Medicine #EDUC4-12751.

AUTHOR CONTRIBUTIONS

L.S., E.C., and E.M. conceived the experiments and wrote the manuscript. L.S., T.M., R.Z., K.L., R.R., Y.-N.L., R.M.-d.-S., A.A., L.L., A.N., and K.H. conducted the experiments. L.S. and E.C. analyzed data and performed statistical analyses. E.C. and E.M. designed the study and provided funding to support the study.

DECLARATION OF INTERESTS

The authors report no relevant conflicts.

INCLUSION AND DIVERSITY

We support inclusive, diverse, and equitable conduct of research. One or more of the authors of this paper self-identifies as an underrepresented ethnic minority in science.

Received: March 1, 2022
Revised: August 18, 2022
Accepted: November 19, 2022
Published: December 20, 2022

(D) miRNome heatmap analysis of miRNA expression demonstrate a robust change 24 h after transfection with *VEGF-A* chemically modified mRNA (middle left). Volcano plot representing the most upregulated and downregulated miRs indicated that miR-6316 is highly upregulated after *VEGF-A* chemically modified RNA transfection.

(E) A representative experimental overview of *VEGF-A* chemically modified mRNA transfection with a co-transfection of antagomiRs against upregulated miRs (middle center).

(F) Representative VEGF-A 3′ UTR luciferase assay results quantified by percentage of firefly/Renilla luciferase activity compared with no-insert control. Experimental conditions were as follows: no insert, control untransfected, and miR-106b-5p mimic transfections (middle right) (n = 4 no insert, n = 4 control untransfected, and n = 4 miR-106b-5p mimic tranfections [biological replicates]).

(G) Representative western blot demonstrating sustained VEGF-A protein expression by co-transfecting NRVMs with *VEGF-A* chemically modified mRNA and antagomiRs. Quantification by densitometry analysis (left bottom) (n = 9 in anti-miR-6316 and miR cocktail and n = 7 in *EGFP* chemically modified mRNA [biological replicates]).

Data are represented as mean ± SEM. Statistical significance was determined using an independent t test.

REFERENCES

1. Cingolani, E., Goldhaber, J.I., and Marbán, E. (2018). Next-generation pacemakers: from small devices to biological pacemakers. Nat. Rev. Cardiol. *15*, 139–150.
2. DiFrancesco, D. (1986). Characterization of single pacemaker channels in cardiac sino-atrial node cells. Nature *324*, 470–473.
3. Epstein, A.E., DiMarco, J.P., Ellenbogen, K.A., Estes, N.A.M., 3rd, Freedman, R.A., Gettes, L.S., Gillinov, A.M., Gregoratos, G., Hammill, S.C., Hayes, D.L., et al. (2013). 2012 ACCF/AHA/HRS focused update incorporated into the ACCF/AHA/HRS 2008 guidelines for device-based therapy of cardiac rhythm abnormalities: a report of the American college of cardiology foundation/American heart association task force on practice guidelines and the heart rhythm society. J. Am. Coll. Cardiol. *61*, e6–e75.
4. Cho, H.C., and Marbán, E. (2010). Biological therapies for cardiac arrhythmias: can genes and cells replace drugs and devices? Circ. Res. *106*, 674–685.
5. Rosen, M.R., Brink, P.R., Cohen, I.S., and Robinson, R.B. (2004). Genes, stem cells and biological pacemakers. Cardiovasc. Res. *64*, 12–23.
6. Miake, J., Marbán, E., and Nuss, H.B. (2002). Biological pacemaker created by gene transfer. Nature *419*, 132–133.
7. Kapoor, N., Liang, W., Marbán, E., and Cho, H.C. (2013). Direct conversion of quiescent cardiomyocytes to pacemaker cells by expression of Tbx18. Nat. Biotechnol. *31*, 54–62.
8. Müller, O.J., Leuchs, B., Pleger, S.T., Grimm, D., Franz, W.-M., Katus, H.A., and Kleinschmidt, J.A. (2006). Improved cardiac gene transfer by transcriptional and transductional targeting of adeno-associated viral vectors. Cardiovasc. Res. *70*, 70–78.
9. Anderson, B.R., Muramatsu, H., Nallagatla, S.R., Bevilacqua, P.C., Sansing, L.H., Weissman, D., and Karikó, K. (2010). Incorporation of pseudouridine into mRNA enhances translation by diminishing PKR activation. Nucleic Acids Res. *38*, 5884–5892. https://doi.org/10.1093/nar/gkq347.
10. Sahin, U., Karikó, K., and Türeci, Ö. (2014). mRNA-based therapeutics—developing a new class of drugs. Nat. Rev. Drug Discov. *13*, 759–780.
11. Magadum, A., Kaur, K., and Zangi, L. (2019). mRNA-based protein replacement therapy for the heart. Mol. Ther. *27*, 785–793.
12. Warren, L., Manos, P.D., Ahfeldt, T., Loh, Y.-H., Li, H., Lau, F., Ebina, W., Mandal, P.K., Smith, Z.D., Meissner, A., et al. (2010). Highly efficient reprogramming to pluripotency and directed differentiation of human cells with synthetic modified mRNA. Cell Stem Cell *7*, 618–630.
13. Karikó, K., Buckstein, M., Ni, H., and Weissman, D. (2005). Suppression of RNA recognition by Toll-like receptors: the impact of nucleoside modification and the evolutionary origin of RNA. Immunity *23*, 165–175.
14. Karikó, K., and Weissman, D. (2007). Naturally occurring nucleoside modifications suppress the immunostimulatory activity of RNA: implication for therapeutic RNA development. Curr. Opin. Drug Discov. Devel. *10*, 523–532.
15. Zangi, L., Lui, K.O., Von Gise, A., Ma, Q., Ebina, W., Ptaszek, L.M., Später, D., Xu, H., Tabebordbar, M., Gorbatov, R., et al. (2013). Modified mRNA directs the fate of heart progenitor cells and induces vascular regeneration after myocardial infarction. Nat. Biotechnol. *31*, 898–907.
16. Sultana, N., Magadum, A., Hadas, Y., Kondrat, J., Singh, N., Youssef, E., Calderon, D., Chepurko, E., Dubois, N., Hajjar, R.J., and Zangi, L. (2017). Optimizing cardiac delivery of modified mRNA. Mol. Ther. *25*, 1306–1315.
17. Kondrat, J., Sultana, N., and Zangi, L. (2017). Synthesis of modified mRNA for myocardial delivery. In Cardiac Gene Therapy (Springer), pp. 127–138.
18. Christoffels, V.M., Grieskamp, T., Norden, J., Mommersteeg, M.T.M., Rudat, C., and Kispert, A. (2009). Tbx18 and the fate of epicardial progenitors. Nature *458*, E8–E9. discussion E9-10.
19. Kapoor, N., Galang, G., Marbán, E., and Cho, H.C. (2011). Transcriptional suppression of connexin43 by TBX18 undermines cell-cell electrical coupling in postnatal cardiomyocytes. J. Biol. Chem. *286*, 14073–14079.
20. Ye, Z., Jin, H., and Qian, Q. (2015). Argonaute 2: a novel rising star in cancer research. J. Cancer *6*, 877–882.
21. Madsen, C., Hooper, I., Lundberg, L., Shafagati, N., Johnson, A., Senina, S., de la Fuente, C., Hoover, L.I., Fredricksen, B.L., Dinman, J., et al. (2014). Small molecule inhibitors of Ago2 decrease Venezuelan equine encephalitis virus replication. Antiviral Res. *112*, 26–37.
22. Hammond, S.M. (2015). An overview of microRNAs. Adv. Drug Deliv. Rev. *87*, 3–14.
23. Laughner, J.I., Ng, F.S., Sulkin, M.S., Arthur, R.M., and Efimov, I.R. (2012). Processing and analysis of cardiac optical mapping data obtained with potentiometric dyes. Am. J. Physiol. Heart Circ. Physiol. *303*, H753–H765.
24. Hu, Y.-F., Dawkins, J.F., Cho, H.C., Marbán, E., and Cingolani, E. (2014). Biological pacemaker created by minimally invasive somatic reprogramming in pigs with complete heart block. Sci. Transl. Med. *6*, 245ra94.
25. Dawkins, J.F., Hu, Y.-F., Valle, J., Sanchez, L., Zheng, Y., Marbán, E., and Cingolani, E. (2019). Antegrade conduction rescues right ventricular pacing-induced cardiomyopathy in complete heart block. J. Am. Coll. Cardiol. *73*, 1673–1687.
26. Protze, S.I., Liu, J., Nussinovitch, U., Ohana, L., Backx, P.H., Gepstein, L., and Keller, G.M. (2017). Sinoatrial node cardiomyocytes derived from human pluripotent cells function as a biological pacemaker. Nat. Biotechnol. *35*, 56–68.
27. Lee, M., Rentz, J., Han, S.O., Bull, D.A., and Kim, S.W. (2003). Water-soluble lipopolymer as an efficient carrier for gene delivery to myocardium. Gene Ther. *10*, 585–593.
28. Sultana, N., Hadas, Y., Sharkar, M.T.K., Kaur, K., Magadum, A., Kurian, A.A., Hossain, N., Alburquerque, B., Ahmed, S., and Chepurko, E. (2020). Optimization of 5′ untranslated region of modified mRNA for use in cardiac or hepatic ischemic injury. Mol. Ther. Methods Clin. Dev. *17*, 622–633.
29. Harcourt, E.M., Kietrys, A.M., and Kool, E.T. (2017). Chemical and structural effects of base modifications in messenger RNA. Nature *541*, 339–346.
30. Kogut, I., McCarthy, S.M., Pavlova, M., Astling, D.P., Chen, X., Jakimenko, A., Jones, K.L., Getahun, A., Cambier, J.C., Pasmooij, A.M.G., et al. (2018). High-efficiency RNA-based reprogramming of human primary fibroblasts. Nat. Commun. *9*, 745.
31. Ramunas, J., Yakubov, E., Brady, J.J., Corbel, S.Y., Holbrook, C., Brandt, M., Stein, J., Santiago, J.G., Cooke, J.P., and Blau, H.M. (2015). Transient delivery of modified mRNA encoding TERT rapidly extends telomeres in human cells. FASEB J. *29*, 1930–1939.
32. Schlaeger, T.M., Daheron, L., Brickler, T.R., Entwisle, S., Chan, K., Cianci, A., DeVine, A., Ettenger, A., Fitzgerald, K., Godfrey, M., et al. (2015). A comparison of non-integrating reprogramming methods. Nat. Biotechnol. *33*, 58–63.
33. Soyombo, A.A., Wu, Y., Kolski, L., Rios, J.J., Rakheja, D., Chen, A., Kehler, J., Hampel, H., Coughran, A., and Ross, T.S. (2013). Analysis of induced pluripotent stem cells from a BRCA1 mutant family. Stem Cell Rep. *1*, 336–349.
34. Li, S.-M., Wu, H.-L., Yu, X., Tang, K., Wang, S.-G., Ye, Z.-Q., and Hu, J. (2018). The putative tumour suppressor miR-1-3p modulates prostate cancer cell aggressiveness by repressing E2F5 and PFTK1. J. Exp. Clin. Cancer Res. *37*, 219.
35. Zhu, F.J., Li, J.Z., and Wang, L.L. (2020). MicroRNA-1-3p inhibits the growth and metastasis of ovarian cancer cells by targeting DYNLT3. Eur. Rev. Med. Pharmacol. Sci. *24*, 8713–8721.
36. Zhang, H., Zhang, Z., Gao, L., Qiao, Z., Yu, M., Yu, B., and Yang, T. (2019). miR-1-3p suppresses proliferation of hepatocellular carcinoma through targeting SOX9. OncoTargets Ther. *12*, 2149–2157.
37. Malumbres, M., and Barbacid, M. (2009). Cell cycle, CDKs and cancer: a changing paradigm. Nat. Rev. Cancer *9*, 153–166.
38. Sekar, R.B., Kizana, E., Cho, H.C., Molitoris, J.M., Hesketh, G.G., Eaton, B.P., Marbán, E., and Tung, L. (2009). I K1 heterogeneity affects genesis

and stability of spiral waves in cardiac myocyte monolayers. Circ. Res. *104*, 355–364.

39. Golden, H.B., Gollapudi, D., Gerilechaogetu, F., Li, J., Cristales, R.J., Peng, X., and Dostal, D.E. (2012). Isolation of cardiac myocytes and fibroblasts from neonatal rat pups. In Cardiovascular Development (Springer), pp. 205–214.
40. Rogers, R.G., Fournier, M., Sanchez, L., Ibrahim, A.G., Aminzadeh, M.A., Lewis, M.I., and Marbán, E. (2019). Disease-modifying bioactivity of intravenous cardiosphere-derived cells and exosomes in mdx mice. JCI insight *4*. e130202.
41. Robinson, M.D., McCarthy, D.J., and Smyth, G.K. (2010). edgeR: a Bioconductor package for differential expression analysis of digital gene expression data. Bioinformatics *26*, 139–140.
42. Yang, B., Lin, H., Xiao, J., Lu, Y., Luo, X., Li, B., Zhang, Y., Xu, C., Bai, Y., Wang, H., et al. (2007). The muscle-specific microRNA miR-1 regulates cardiac arrhythmogenic potential by targeting GJA1 and KCNJ2. Nat. Med. *13*, 486–491.
43. Mesquita, T., Zhang, R., Cho, J.H., Zhang, R., Lin, Y.-N., Sanchez, L., Goldhaber, J.I., Yu, J.K., Liang, J.A., Liu, W., et al. (2022). Mechanisms of sinoatrial node dysfunction in heart failure with preserved ejection fraction. Circulation *145*, 45–60.
44. Rickert, C., and Proenza, C. (2017). ParamAP: standardized parameterization of sinoatrial node myocyte action potentials. Biophys. J. *113*, 765–769.
45. Justus, C.R., Leffler, N., Ruiz-Echevarria, M., and Yang, L.V. (2014). In vitro cell migration and invasion assays. J. Vis. Exp., 51046. https://doi.org/10.3791/51046.
46. Chen, L., Wang, Y., Jiang, W., Ni, R., Wang, Y., and Ni, S. (2020). CDK14 involvement in proliferation migration and invasion of esophageal cancer. Ann. Transl. Med. *8*, 559.
47. Yang, Y., Yuan, G., Xie, H., Wei, T., Zhu, D., Zhu, Y., and Zheng, S. (2021). CDK14 expression is elevated in patients with non-small cell lung cancer and correlated with poor prognosis. J. Int. Med. Res. *49*. 03000605211013199.
48. Cho, J.H., Zhang, R., Kilfoil, P.J., Gallet, R., de Couto, G., Bresee, C., Goldhaber, J.I., Marbán, E., and Cingolani, E. (2017). Delayed repolarization underlies ventricular arrhythmias in rats with heart failure and preserved ejection fraction. Circulation *136*, 2037–2050.
49. Cho, J.H., Kilfoil, P.J., Zhang, R., Solymani, R.E., Bresee, C., Kang, E.M., Luther, K., Rogers, R.G., de Couto, G., Goldhaber, J.I., et al. (2018). Reverse electrical remodeling in rats with heart failure and preserved ejection fraction. JCI insight *3*. e121123.

STAR★METHODS

KEY RESOURCES TABLE

REAGENT or RESOURCE	SOURCE	IDENTIFIER
Antibodies		
Rabbit Polyclonal anti-TBX18	LifeSpan Biosciences	Cat# LS-B5638-100 RRID: AB_2924708
Rabbit Polyclonal anti-TBX18	Abcam	Cat # ab115262 RRID: AB_2924709
Rabbit Polyclonal anti-Connexin 43	Sigma -Aldrich	Cat# C6219 RRID: AB_476857
Rabbit Polyclonal anti-GAPDH	Cell Signaling	Cat#5174T RRID: AB_2924710
Rabbit Monoclonal anti-alpha-Actinin	Abcam	Cat# ab9465 RRID: AB_307264
Mouse Monoclonal anti-PFTAIRE	Santa Cruz Biotechnology	Cat# sc-376366 RRID: AB_10988257
Mouse Monoclonal anti-E2F-5	Santa Cruz Biotechnology	Cat# sc-374268 RRID: AB_10988935
Rabbit Polyclonal anti-HCN4	Alomone Labs	Cat# APC-052 RRID: AB_2039906
Rabbit Polyclonal anti-HCN2	Alomone Labs	Cat# APC-030 RRID: AB_2313726
Mouse Monoclonal anti-Connexin 45	Abcam	Cat# Ab78408 RRID: AB_1566083
Goat Polyclonal anti-Rabbit IgG, HPR-linked Antibody	Cell Signaling	Cat# 7074 RRID: AB_2099233
Goat Anti-rabbit Alexa Fluor 488	Thermo Fisher Scientific	Cat# A-11008 RRID: AB_143165
Goat Anti-rabbit Alexa Fluor 647	Thermo Fisher Scientific	Cat# A32733 RRID: AB_2633282
Goat Anti-Mouse Alexa Fluor 594	Thermo Fisher Scientific	Cat# A-11005 RRID: AB_2534073
Bacterial and virus strains		
Ad-CMV-TBX18-IRES-GFP	Kapoor et al.,2013	N/A
Chemicals, peptides, and recombinant proteins		
Acriflavine	Sigma-Aldrich	Cat# A8126-25G
Lipofectamine RNAiMax	Thermo Fisher	Cat# 13778150
DharmaFECT	Horizon Discovery	Cat# T-2001-04
RH237 Voltage-sensitive dye	Invitrogen	Cat# S1109
Blebbistatin	Sigma-Aldrich	Cat# B0560-5MG
Methyl Green-Pyronin stain	Sigma-Aldrich	Cat# HT70
Signal Stain Boost IHC Detection (HRP mouse)	Cell Signaling	Cat# 8125
Signal Stain Antibody Diluent	Cell Signaling	Cat# 8112S
Scotts tap water substrate	Sigma-Aldrich	Cat# S5134
Hematoxylin Solution	Sigma-Aldrich	Cat# 1051752500
Eosin Y solution	Sigma-Aldrich	Cat# HT110280
Critical commercial assays		
Pierce DAB Substrate Kit	Thermo Fisher	Cat# PI34002
Dual Luciferase reporter Assay	Promega	Cat# E2940

(*Continued on next page*)

Continued

REAGENT or RESOURCE	SOURCE	IDENTIFIER
Click-iT Plus EdU Alexa 594	Thermo Fisher	Cat# C10639
Click-iT Plus EdU Alexa 488	Thermo Fisher Scientific	Cat# C10337
High-Capacity cDNA Reverse Transcription kit	Thermo Fisher Scientific	Cat# 4387406
RNeasy plus Kit	Qiagen	Cat# 74134
TaqMan Fast Advanced Master Mix	Thermo Fisher Scientific	Cat# 4444964
TaqMan probes	Thermo Fisher Scientific	Table S3 in the supplement
Deposited data		
Processed miRNA seq data (TBX18)	This paper	Mendeley Data, V1, https://doi.org/10.17632/d3d488fj8n.1
Processed miRNA seq data (VEGF-A)	This paper	S Mendeley Data, V1, https://doi.org/10.17632/d3d488fj8n.1
Raw data from Figures 1–4 were deposited on Mendeley	This paper	Mendeley Data, V1, https://doi.org/10.17632/d3d488fj8n.1
Raw Western blot images from Figures 1–4 were deposited on Mendeley	This paper	Mendeley Data, V1, https://doi.org/10.17632/d3d488fj8n.1
Experimental models: Cell lines		
Neonatal rat Ventricular myocyte isolation (NRVMs)	Sekar et al.,2009	N/A
A549 Human Lung Carcinoma	Sigma-Aldrich	Cat# 86012804
SKOV-3 Human Ovarian Carcinoma	ATCC	Cat# HTB-7
769-P Human Adenocarcinoma Renal	ATCC	Cat# CRL-1933
HEK 293TN	System Biosciences	Cat# LV900-A1
Experimental models: Organisms/strains		
Female Sprague-Dawley rats	Charles River Laboratories	N/A
Oligonucleotides		
N1-methylpseudo-U-Tbx18	This paper Trilink	lot# C3-D01A
5-methoxy-U-Tbx18	This paper Trilink	lot# C3-D02A
N1-methylpseudo-U-eGFP	This paper Trilink	lot# C3-D03A
N1-mehtylpseudo-U-VEGF-A	This paper Trilink	lot# C3-D04A
miR-1-3p/1b target site vector	This paper Promega	N/A
miR-Hairpin inhibitors/mimics	This paper Dharmacon	Table S2 in the supplement
miRs 3′UTR target sites	This paper	Table S1 in the supplement
Recombinant DNA		
pmiR-GLO vector	Yang et al.,2018 Promega	Cat#E1330
pmiR-target vector (VEGF-A)	OriGene	Cat# SC217124
pmiR-GLO-TBX18 3′UTR-miR-1-3p	This paper Promega	N/A
Software and algorithms		
MATLAB Rhythm	Laughner et al., 2012	https://www.mathworks.com/products/matlab.html
Powerlab	ADInstruments Inc	https://www.adinstruments.com/products/powerlab/c?creative
Lab Chart 7Pro	ADInstruments Inc	https://www.adinstruments.com/products/labchart
GraphPad prism 9	GraphPad	https://www.graphpad.com/scientific-software/prism/

(*Continued on next page*)

Continued

REAGENT or RESOURCE	SOURCE	IDENTIFIER
ImageJ	N/A	https://imagej.nih.gov/ij/index.html
Image Lab v6.0 software	BioRad	https://www.bio-rad.com/en-us/product/image-lab-softwar/
Other		
Falcon Permeable Support for 12-well 8.0μM PET	Corning	Cat# 353182

RESOURCE AVAILABILITY

Lead contact

Further information and requests for resources and reagents should be directed to the lead contact, Eugenio Cingolani (eugenio.cingolani@csmc.edu).

Materials availability

All unique/stable reagents generated in this study are available from the lead contact with a completed materials transfer agreement.

Data and code availability

- All data generated in this manuscript have been deposited at Mendeley and are publicly available as of the date of publication. Accession numbers are listed in the key resources table. Microscopy data reported in this paper will be shared by the lead contact upon request.
- This paper does not report original code.
- Any additional information required to reanalyze the data reported in this paper is available from the lead contact upon request.

EXPERIMENTAL MODEL AND SUBJECT DETAILS

Rats

Female Sprague-Dawley rats (weight, 400–428g; Charles River Laboratories) were used in this study. n = 3 rats per group were used for *in vivo* experiments. All animal husbandry was performed in accordance to guidelines set by Cedars-Sinai Medical Center's Institutional Animal Care and Use Committee. Rats were euthanized by isoflurane overdose and vital organ harvest. All experimental procedures were approved by Cedars-Sinai Medical Center's Institutional Animal Care and Use Committee.

Cells

Neonatal Rat Ventricular Myocytes (NRVMs) were isolated from 1-2 day-old neonatal rat pups as described previously[7,19,38,39] and plated at a density of 200,000 cells per well of a 6-well culture dish. NRVMs were cultured in Media 199 (GIBCO) supplemented with the following: 1% HEPES Buffer solution (GIBCO), 1% MEM non-essential amino acids (GIBCO), 1.75g Glucose, 1% 200 mM L-glutamine (GIBCO), 10% or 2% heat inactivated fetal bovine serum (GE Healthcare). SKOV-3 cells (ATCC) were cultured in McCoy's 5A medium (ATCC) supplemented with 10% heat inactivated fetal bovine serum (GE Healthcare). 769-P cells (ATCC) were cultured in RPMI-1640 media (ATCC) supplemented with 10% heat inactivated fetal bovine serum (GE Healthcare). A549 cells (Sigma-Aldrich) were cultured in Dulbecco's Modified Eagle's Medium/Nutrient Mixture F-12 Ham media (Sigma-Aldrich) supplemented with 10% heat inactivated fetal bovine serum (GE Healthcare).

METHOD DETAILS

Synthesis of TBX18, VEGF-A, and eGFP CMmRNA

CMmRNAs were designed with a full substitution of 1-methylpseudouridine-5′-triphosphate capped (Cap 1) and 5-methoxy-U using CleanCap™ AG, polyadenylated (120A), purified using silica membrane with DNase and phosphatase treatment, and packaged as a solution in 1mM sodium citrate, pH 6.4 (TriLink Biotechnologies).

In vitro CMmRNA transfection

One day prior to all transfections, serum concentration of NRVM media was reduced from 10% to 2%. The day of transfections 3ug of 1-methylpseudo-U CMm*TBX18*, 5-methoxy-U CMm*TBX18*, 1-methylpseudo-U CMm*VEGF-A*, and negative control 1-methylpseudo-U CMm*eGFP* were diluted in 50ul of Opti-MEM medium (Thermo Scientific). Lipofectamine RNAiMAx transfection reagent (Life technologies) was prepared according to the manufacturer's protocol. The mixture was incubated for 20 min at room

temperature and then added (in dropwise) to cells.[17] Positive control (Adenovirus encoding TBX18) was added to the NRVMs as previously described.[7,19] Twerty-four and 48h post-transfection/transduction RNA and protein was collected. For repeated transfections, CMmRNA was delivered at 24h intervals for a total of 5 days using the described transfection method. To block Argonaute 2 function, 2.5μM of Acriflavine (Sigma) was added to NRVM culture media 1 day prior to transfections and daily throughout the 72h time point. In co-transfection experiments using CMmRNA and miRIDIAN miR hairpin inhibitors, 10uM antagomiR (Dharmacon; Table S2 in the Supplement) were used.

RNA purification, RT-qPCR analysis, and RNA sequencing

Total or small RNA was purified as previously described[40] using the RNeasy plus Mini kit (Qiagen), respectively, according to manufacturer's protocol. Eight-hundred (*in vitro*) and 1,000 (*in vivo*) nanograms of RNA was used for cDNA synthesis (High-Capacity cDNA Reverse transcription kit Thermo Scientific). Fifty nanograms of cDNA was then amplified using TaqMan probes (Table S3 in the Supplement) and TaqMan gene expression master mix (Thermo Scientific). Cycling conditions were performed as follows: Step 1: 25°C for 10 min, Step 2: 37°C for 120 min and Step 3: 85°C for 5 min. The $2^{-\Delta\Delta Ct}$ method was used to determine gene expression fold change. For RNA sequencing, miR count was calculated using the QIAseq-miRNA platform (http://ngsdataanalysis.sabiosciences.co-m/QIAseqmiRNA/). Trimmed mean of M-values to normalize gene expression was carried out using the EdgeR[41] package for Bioconductor. The cutoff of differential miR was a fold-change threshold of 1.5 and maximum p value of 0.05. The miRNome upregulated in CMm*TBX18* and CMm*VEGF-A* was aligned to the 3′UTR using TargetScan and miRmap (Table S1 in the Supplement).

Luciferase assay

Luciferase construct was designed as previously described.[42] Briefly, a 42 base pair *TBX18* 3′UTR segment (sense 5′-aaac -ta -gcggccgc- tagt-CCCCTTGACTAGTAAACATTCCA-t-3′ and antisense 5′-ctagaTGGAATGTTTACTAGTCAAGGGGacta-gcggccgc-tagttt-3′) containing the putative miR-1-3p/miR-1b target site was cloned into the PmeI and XbaI sites of a pmiRGLO vector (Promega). For pmirGLO-TBX18 3′UTR-miR-1-3p-target-mutant segment (sense 5′- AAACTAGCGGCCGCTAGTCCCCTTGACTAG TAATGTAAGGAT-3′ and antisense 5′- CTAGATCCTTATATTACTAGTCAAGGGGACTAGCGGCCGCTAGTTT-3′), the miR-1-3p target site (ACATTCC) within the *TBX18* 3′UTR was mutated to (TGTAAGG). Per the manufacturer's protocol (Promega), HEK293 cells were seeded into 96-well plates and co-transfect with either miR-1-3p mimic (Dharmacon) or miRNA Mimic negative control (ThermoFishier), with either pmirGLO-TBX18-3′UTR-miR-1-3p-target or pmirGLO-TBX18-3′UTR-miR-1-3p-target-mutant luciferase reporter vector using DharmaFECT (Horizon Discovery) for two days. After two days, an assessment of the luciferase activity was made using the Dual-Luciferase Reporter Assay (Promega). Firefly luciferase activity was normalized by renilla luciferase activity and expressed as a percentage of the control (n = 4). 3′UTR clone of vascular endothelial grown factor A (VEGF-A) was commercially purchased (ORIGENE) and the miRIDIAN miR hairpin mimic 106b-5p (Dharmacon) were conducted as previously described.

Immunoblotting

Radio Immuno-Precipitation Assay (RIPA) lysis buffer (Thermo Scientific) supplemented with protease/phosphatase inhibitor cocktail and EDTA (Thermo Scientific) was added to the six well plate. Lysates were then sonicated while the samples were kept on ice. The lysate was then centrifuged at 14,000 × g for 15 min at 4°C and the pellet was discarded. The total protein concentration of the supernatant was measured using a bicinchoninic acid (BCA) assay (Thermo Scientific). Protein samples were prepared for denaturing gel electrophoresis by adding LDS and DTT. For *in vitro* assay 15μg of protein and for *in vivo* 25μg of protein was loaded in a 4–12% Bis Tris SDS polyacrylamide gel (Novex) at 175V for 120min. Proteins were immobilized on a PVDF (Thermo Scientific) membrane using wet transfer method (Bio-Rad) at 80V for 120min. Membranes were blocked for 1 h at room temperature in 5% non-fat dried milk (Bio-Rad) and then incubated overnight in primary antibodies diluted in blocking solution at 4°C with shaking. Following the overnight incubation, membranes were washed with TBST-T (3 × 10min) and then probed with Alexa Fluor secondary antibodies for 1 h at room temperature. After secondary antibody incubation, membranes were washed with TBS-T (3 × 10min) and then fluorophores were fixed in methanol for 1min and allowed to dry in the dark. For HRP-linked secondary antibodies, membranes were incubated for 120s in enhanced chemiluminescent solution (Thermo Scientific) and immunoreactivity was visualized using a ChemiDoc (Bio-Rad). Densitometry was used to quantify protein abundance using ImageLab v6.0 software (Bio-Rad). Due to local differences in background noise, some non-expressed proteins resulted in a negative value when normalized. All negative values were arbitrarily set to zero.

Single cell electrophysiology

Whole-cell electrophysiology recordings were performed as we previously described[43] Experiments were carried out using standard microelectrode amphotericin B-perforated whole-cell patch-clamp with an Axopatch 200B amplifier (Molecular Devices) with a sampling rate of 20 kHz and low-pass filtered at 5 kHz. Experiments were performed at 36 ± 1°C with cells perfused with an extracellular Tyrode's solution containing (mM): 140 NaCl, 5 KCl, 1.8 CaCl2, 1 MgCl2, 10 glucose, and 10 HEPES, pH 7.4 NaOH. Microelectrodes with tip resistances of 3.5–6 MΩ were backfilled with intracellular pipette solution containing (mM): 130 KCl, 10 NaCl, 1 $MgCl_2$, 5 Mg-ATP, 5 creatine phosphate, 10 HEPES, and 250 μg/mL amphotericin B; pH 7.2 KOH. Action potentials were recorded using I = 0 mode in whole-cell recording configuration. AP parameters were calculated using ParamAP, as described[44].

5-Ethynyl-2′-deoxyuridine (EdU assay)

Click-iT EdU cell proliferation assay (Thermo Fisher): SKOV-3, 769-P, and A549 cells were cultured in Nunc Lab-Tek II 8 chamber slides (Thermo Fisher) at a density of 50,000 cells per chamber slide. One day before the transfections, serum concentration was reduced from 10 to 2%. On the day of transfections, 800ng of 1-methylpseudo-U CMm*TBX18*, CMme*GFP*, and CMm*Tbx18* only and for co-transfection experiments using CMmRNA and miRIDIAN miR hairpin inhibitors and mimics, 1uM antagomir/mimics (Dharmacon; Table S2 in the Supplement) were diluted in 50ul of Opti-Mem medium (Thermo Scientific). Lipofectamine RNAiMAx transfection reagent (Life technologies) was prepared according to the manufacturer's protocol. The mixture was incubated for 20 min at room temperature and then added (dropwise) to cells. For the following group, Lipofectamine, only the identical incubation of 20min was followed and added (in dropwise) to cells. 72h later, 10mM of EdU stock solution was prepared in 5mL of prewarmed media to make 20μM EdU labeling solution final concentration per chamber slide was 10μM, and the cells were incubated for 2h in 37°C incubators. After incubation, Fixation, and permeabilization were followed, 3.7% formaldehyde was used to fixate under 15 min at room temperature, and cells were then washed twice in 500ul of 3% BSA in PBS. After the wash, cells were permeabilized in 0.5% Triton X-100 in PBS and incubated for 20 min at room temperature. After the 20min incubation, 500ul of 1x Click-it EdU buffer cocktail was added Alexa Fluor 488 and Alexa Fluor 594 for the CMme*GFP* transfection (1x Click-it EdU buffer cocktail was prepared according to manufacturer's protocol), and cells were imaged using a multi-photon confocal fluorescence microscope (Leica).

Transwell migration assay

Falcon Permeable 12 well plate with 8.0μM transparent polyester (PET) membrane transwell chamber slides/plates were used (Sigma-Aldrich) for this assay. 40,000 cells (A549, SKOV-3 and 769-p) were transfected in suspension following the described transfection protocol and seeded in the upper chambers in serum-free media. The chemoattractant was added in the lower chamber (10% FBS A549, SKOV-3 and 769-p media). 72h later, the cells were fixed in methanol and stained with 0.5% crystal violet following the described protocol.[45] Four visual fields were selected randomly, and imaged under a light microscope. Migrated cells were counted using the described analysis.[45]

Immunostaining

NRVMs were fixed 72h post-transfection with 4% paraformaldehyde, washed (3 × 3min) with PBS, permeabilized with 0.1% Triton X-100, washed (3 × 3min) with PBS, and then blocked (Protein block, serum free). Following protein block, NRVMs were incubated with primary antibodies. After the overnight incubation at 4°C, NRVMs were then washed (3 × 3min) with PBS, and incubated with the appropriate Alexa Fluor secondary antibodies for 1 h at room temperature, washed (3 × 3min) in PBS, and then mounted with Fluoroshield with DAPI (Sigma). Immunostained NRVMs were imaged using a multi-photon confocal fluorescence microscope (Leica). Sprague Dawley organ sections (injection site, lungs, liver, kidney, and spleen) were frozen using OCT and flash freezing in 2-methyl butane and liquid nitrogen. Sections were sectioned at 6μM using Leica cryosectioning. Fixation was performed using 4% paraformaldehyde for 10 min at room temperature. Sections were washed 2-times with PBS for 5min. Sections were quenched using methanol/peroxidase for 10 min at room temperature and washed 2-time with PBS for 5min. Blocking solution was added to the sections for 1 h, followed by CDK14 (PFTAIRE-1) 1/100 dilution and E2F-5 1/100 dilution (Santa Cruz) and incubated overnight. Antibody was removed by washing 2-times in PBS for 5min, and 2-drops of Signalstain Boost detection reagent was added HRP, mouse (Cell Signaling) and incubated in a humidified chamber for 30 min at room temperature. Sections were washed 3-times with PBS for 5min each. DAB (Thermo Fisher) was added and incubated for 7min and counterstained with methyl green-pyronin stain (Sigma Aldrich) for 5min. The sections were rinsed thoroughly in deionized water, dehydrated, and mounted with a DPX-mounting solution. Samples were quantified using the Allred scoring system (insert ciatitons). The total IHC score was calculated as the sum of the scores for staining intensity (0, no staining; 1, weak staining; 2, moderate staining; 3, strong staining) and the percent area of staining (0, 0%–10%; 1, 11%–25%; 2, 26%–50%; 3, 51%–75%; 4, 76–100%). IHC scores of >3 were defined as strong staining and high expression, and scores of ≤3 were defined as weak staining and low expression.[46,47] Hematoxyling and eosin staining was performed by incubating the slides in hematoxyling stain for 10min, rinsing with water, placing them in Scotts for 1min, followed by rinsing with water. Lastly slides were incubated with Eosin Y for 5min and dehydrated by 70%, 95 and 100% ethanol for 1min and DPX mount, and imaged under a light microscope.

In vivo delivery of *TBX18* CMmRNA

CMmRNA *in vivo* transfections were carried out by combining 80μL of RNAiMAx in 5μL of OptiMEM in 1 Eppendorf tube and vortexed. This mixture was incubated at room temperature for 10min as previously described.[17] In another Eppendorf tube, 100μg of CMmRNA, 20μM of miRIDIAN microRNA hairpin inhibitors (rno-mir-1b and rno-mir-1-3p) and 5μL of OptiMEM were added. Both mixtures were combined and incubated at room temperature for 10min. Using a 31G-needle insulin syringe the mixture was injected into the left ventricular apex of Sprague-Dawley rats (weight, ∼400g; Charles River Laboratories). Animals were anesthetized with 4% isoflurane (induction), intubated and placed on a ventilator with a vaporizer supplying 2% isoflurane for the remainder of the surgery. Temperature was kept at 38°C using a heating pad. All animal procedures were approved by the Cedars-Sinai Medical Center Institutional Animal Care and Use Committee (IACUC protocol 9109).

Ex vivo high-resolution voltage mapping and ECG recordings

Anesthetized rats were injected with 1000 U of heparin (i.p.) and quickly euthanized. Hearts were then harvested and perfused with warmed Tyrode's solution containing: 1.8mM $CaCl_2$ 8 mL/min. Hearts were loaded with 10μM voltage-sensitive dye RH237 (Invitrogen) and 10μM blebbistatin (Sigma-Aldrich) to eliminate motion artifacts. High-speed optical voltage mapping images (sampled at 1000 frames/s) were acquired with a MiCAM05 Ultima-L CMOS camera (SciMedia, excitation, 520/35 nm: dichroic, 560nm; emission, 715nm long pass). As previously described.[23,48,49] Optical mapping data were analyzed through a MATLAB Rhythm software kindly provided by Dr. Igor Effimov.[23] Hearts remained immersed in Tyrode's solution and surface ECG was continuously recorded (Powerlab, ADInstruments Inc.) by electrodes placed inside the bath. ECG raw data were analyzed using a dedicated software (Lab Chart 7 PRO; AD Instruments). Atrioventricular (AV) block was induced surgically (*ex vivo*) by cutting the septum just below the AV node region. Complete AV block was confirmed by visual inspection of ECG signals demonstrating AV dissociation.

QUANTIFICATION AND STATISTICAL ANALYSIS

Data are represented as means ± SEM. Statistical significance was determined by independent t-tests or one-way ANOVA(Prism GraphPad v9). A p value ≤ 0.05 was considered statistically significant.